

# Probe-Seq enables transcriptional profiling of specific cell types from heterogeneous tissue by RNA-based isolation

Ryoji Amamoto<sup>1</sup> Mauricio D. Garcia<sup>1</sup> Emma R. West<sup>1</sup> Jiho Choi<sup>1</sup> Sylvain W. Lapan<sup>1</sup> Elizabeth A. Lane<sup>2</sup>  
Norbert Perrimon<sup>2</sup> Constance L. Cepko<sup>1,\*</sup>

<sup>1</sup>Department of Genetics and Ophthalmology, Howard Hughes Medical Institute, Blavatnik Institute, Harvard Medical School, Boston MA 02115, USA.

<sup>2</sup>Department of Genetics, Howard Hughes Medical Institute, Blavatnik Institute, Harvard Medical School, Boston MA 02115, USA.

\*Corresponding author: Constance L. Cepko (cepko@genetics.med.harvard.edu).

## 0 ABSTRACT

1 **Recent transcriptional profiling technologies are uncovering**  
2 **previously-undefined cell populations and molecular mark-**  
3 **ers at an unprecedented pace. While single cell RNA**  
4 **(scRNA) sequencing is an attractive approach for unbiased**  
5 **transcriptional profiling of all cell types, a complementary**  
6 **method to isolate and sequence specific cell populations from**  
7 **heterogeneous tissue remains challenging. Here, we devel-**  
8 **oped Probe-Seq, which allows deep transcriptional profiling**  
9 **of specific cell types isolated using RNA as the defining fea-**  
10 **ture. Dissociated cells are labelled using fluorescent *in situ***  
11 **hybridization (FISH) for RNA, and then isolated by fluores-**  
12 **cent activated cell sorting (FACS). We used Probe-Seq to pu-**  
13 **rify and profile specific cell types from mouse, human, and**  
14 **chick retinas, as well as the *Drosophila* midgut. Probe-Seq**  
15 **is compatible with frozen nuclei, making cell types within**  
16 **archival tissue immediately accessible. As it can be multi-**  
17 **plexed, combinations of markers can be used to create speci-**  
18 **ficity. Multiplexing also allows for the isolation of multiple**  
19 **cell types from one cell preparation. Probe-Seq should en-**  
20 **able RNA profiling of specific cell types from any organism.**

## 21 INTRODUCTION

22 Multicellular eukaryotic tissues often comprise many differ-  
23 ent cell types, commonly classified using their morphologi-  
24 cal features, physiological function, anatomical location, and/or  
25 molecular markers. For example, the retina, a thin sheet of neu-  
26 ral tissue in the eye that transmits visual information to the brain,  
27 contains seven major cell classes - rods, cones, bipolar cells  
28 (BC), amacrine cells (AC), horizontal cells (HC), Müller glia  
29 (MG), and retinal ganglion cells (RGC), first defined primarily  
30 using morphology<sup>1,2</sup>. More recently, scRNA profiling technolo-  
31 gies have led to the appreciation of many subtypes of these ma-  
32 jor cell classes, bringing the total number of retinal cell types  
33 close to 100<sup>3-5</sup>. Such accelerated discovery of cellular diversity  
34 is not unique to the retina, as scRNA profiling is being carried  
35 out in many tissues and organisms<sup>6-8</sup>.

36 Several approaches have been used to transcriptionally pro-  
37 file tissues. Bulk RNA sequencing of whole tissues can be done  
38 at great depth, but does not capture the diversity of individual  
39 transcriptomes and often fails to reflect signatures of rare cell  
40 types. Currently, bulk sequencing of specific cell types is limited

by the availability of cell type-specific promoters, enhancers,  
dyes, or antigens for their isolation<sup>9-14</sup>. This has limited bulk  
RNA sequencing primarily to select cell types in genetically-  
tractable organisms. Single cell and single nucleus RNA se-  
quencing methods have allowed for the recording of transcrip-  
tional states of many individual cells simultaneously<sup>3,5,15-18</sup>. De-  
spite the undeniable appeal of scRNA sequencing, capturing  
deep profiles of specific cell populations in bulk can be suffi-  
cient or preferable for many experiments, e.g. when the goal is  
to understand the results of perturbations.

We and others have used antibodies to enable FACS-  
based isolation for transcriptional profiling of specific cell  
populations<sup>11,19-23</sup>. However, antibodies are frequently unavail-  
able for a specific cell type. Furthermore, marker proteins in cer-  
tain cell types such as neurons are often localized to processes  
that are lost during cellular dissociation. We therefore aimed to  
create a method that would leverage the newly discovered RNA  
expression patterns for the isolation of specific cell populations  
from any organism. This led us to develop Probe-Seq, which  
uses a FISH method based upon a new probe design, Serial Am-  
plification By Exchange Reaction (SABER)<sup>24</sup>. Probe-Seq uses  
RNA markers expressed in specific cell types to label cells for  
isolation by FACS and subsequent transcriptional profiling. Al-  
though specific cells cultured *in vitro* have been successfully la-  
belled by FISH for isolation using FACS, this method had not  
yet been tested for tissue<sup>25-27</sup>. We used Probe-Seq to isolate  
rare bipolar cells from the mouse retina, cell types that were  
previously defined using scRNA sequencing<sup>5</sup>. We demonstrate  
that probe sets for multiple genes can be hybridized at once,  
allowing isolation of multiple cell types simultaneously. More-  
over, the fluorescent oligonucleotides used to detect the probe  
sets can be quickly hybridized and then stripped. This enables  
isolation of an indefinite number of cell types from one sam-  
ple by serial sorting and re-labeling. We extended Probe-Seq  
to specific bipolar cell subtypes in frozen archival human retina  
by labeling nuclear RNA. To further test the utility of Probe-  
Seq in non-vertebrate animals and non-CNS tissues, we profiled  
intestinal stem cells from the *Drosophila* gut. In each of these  
experiments, the transcriptional profiles of isolated populations  
closely matched those obtained by scRNA sequencing, and in  
most cases, the number of genes detected exceeded 10,000. Fi-  
nally, we used Probe-Seq on the chick retina, an organism that  
is difficult to genetically manipulate, to determine the transcrip-

84 tional profile of a subset of developing retinal cells that give  
85 rise to the chick high acuity area. Taken together, Probe-Seq is  
86 a method that enables deep transcriptional profiling of specific  
87 cell types in heterogeneous tissue from potentially any organ-  
88 ism.

## 89 RESULTS

### 90 Specific bipolar cell subtypes can be isolated and profiled 91 from the mouse retina using Probe-Seq

92 To determine whether Probe-Seq can enable the isolation and  
93 profiling of specific cell types based on FISH labeling, we  
94 tested it using the mouse retina. The retina is a highly het-  
95 erogeneous tissue, with cell classes and subtypes classified by  
96 scRNA sequencing, as well as more classical methods<sup>2</sup>. We  
97 used a new method for FISH, SABER-FISH, to label the in-  
98 tracellular RNA<sup>24</sup>. SABER-FISH uses OligoMiner to design  
99 20-40 nt tiling oligonucleotides that are complementary to the  
100 RNA species of interest and are optimized for minimal off-target  
101 binding. The tiling oligonucleotides are pooled to generate a  
102 gene-specific probe set. Each probe set is then extended using  
103 a primer exchange reaction<sup>28</sup>, which appends many copies of a  
104 short-repeated sequence to each tiling oligonucleotide in the set.  
105 These concatemer sequences can be made unique for each probe  
106 set. The concatemers are detected by the hybridization of short  
107 fluorescent oligonucleotides.

108 To isolate specific BC subtypes, fresh adult mouse retinas  
109 were dissociated, fixed, and permeabilized prior to FISH label-  
110 ing (**Figure 1a**). We designed gene-specific probe sets against  
111 *Vsx2*, a marker of all BCs and MG, and *Grik1*, a marker of  
112 BC2, BC3A, BC3B, and BC4 subtypes (~2% of all retinal  
113 cells)<sup>5</sup> (**Figure 1b**). *Vsx2* and *Grik1* probe sets were hybridized  
114 to the dissociated retinal cells overnight at 43°C, and fluores-  
115 cent oligonucleotides were subsequently hybridized to the gene-  
116 specific probe sets. By FACS, single cells were identified by  
117 gating for a single peak of Hoechst<sup>+</sup> events, while debris and  
118 doublets were excluded (**Figure 1c**). Out of these single cells,  
119 the *Vsx2*<sup>+</sup> population was judged to be the cells that shifted  
120 away from the diagonal *Vsx2*<sup>-</sup> events (**Figure 1c**). Out of the  
121 *Vsx2*<sup>+</sup> population, we found three populations that were *Grik1*<sup>-</sup>,  
122 *Grik1*<sup>MID</sup>, and *Grik1*<sup>HI</sup>. Based upon scRNA sequencing of BC  
123 subtypes, *Grik1*<sup>MID</sup> likely corresponded to BC2, and *Grik1*<sup>HI</sup>  
124 to BC3A, BC3B, and BC4<sup>5</sup>. We isolated both *Grik1*<sup>MID</sup> and  
125 *Grik1*<sup>HI</sup> (henceforth called *Grik1*<sup>+</sup>) cells as well as *Vsx2*<sup>+</sup>/*Grik1*<sup>-</sup>  
126 (henceforth called *Grik1*<sup>-</sup>) and *Vsx2*<sup>-</sup> cell populations. We ex-  
127 pected the *Grik1*<sup>+</sup> population to contain BC2-BC4, the *Grik1*<sup>-</sup>  
128 population to contain other BC subtypes and MG, and the  
129 *Vsx2*<sup>-</sup> population to contain non-BC/MG cell types (**Figure 1d**).  
130 The isolated populations displayed the expected FISH puncta  
131 (**Figure 1e**). On average, we isolated 200,000±0 *Vsx2*<sup>-</sup> cells,  
132 96,000±18,600 *Grik1*<sup>-</sup> cells, and 22,000±1,000 *Grik1*<sup>+</sup> cells per  
133 biological replicate, with each replicate originating from 2 reti-  
134 nas. These results indicate that gene-specific SABER-FISH can  
135 label dissociated cell populations for isolation by FACS.

136 To determine whether the isolated populations corresponded  
137 to the expected cell types, we reversed the crosslinking and ex-  
138 tracted the RNA from these cells. SMART-Seq v.4 cDNA lib-  
139 raries were generated and sequenced on NextSeq 500. Each  
140 sample was sequenced to a mean of 15±3 million 75 bp paired-

141 end reads to be able to reliably detect low abundance tran-  
142 scripts. The average 3' bias for the mapped reads for all samples  
143 was 0.74±0.02, which corresponds to a RNA Integrity Num-  
144 ber (RIN) of 2-4<sup>29</sup>, indicating mild degradation of RNA. Un-  
145 biased hierarchical clustering showed that samples of the same  
146 cell population clustered together (average Pearson correlation  
147 between samples within population:  $r = 0.93$ ) (**Supplementary**  
148 **Figure 1**). The three populations were then analyzed for differ-  
149 ential expression (DE). Between each population, the frequency  
150 distribution of all *p*-values showed an even distribution of null  
151 *p*-values, thus allowing for calculation of adjusted *p*-value using  
152 the Benjamini-Hochberg procedure (**Supplementary Figure 1**).  
153 Between *Grik1*<sup>-</sup> and *Grik1*<sup>+</sup> populations, we found 1,740 differ-  
154 entially expressed genes (adjusted *p*-value < 0.05) out of 17,649  
155 genes (**Supplementary Figure 1**). The high number of genes  
156 detected indicates successful bulk RNA sequencing of low abun-  
157 dance transcripts.

158 To determine which retinal cell types were enriched in the  
159 isolated populations, we cross-referenced the DE gene set (ad-  
160 justed *p*-value < 0.05) to retinal cell class-specific markers  
161 identified by Drop-Seq (see Methods for details of gene set  
162 curation)<sup>3</sup>. We saw that the *Vsx2*<sup>-</sup> population was enriched for  
163 markers of all cell classes except for BCs and MG (**Supple-**  
164 **mentary Figure 2**), as expected from the expression pattern  
165 of *Vsx2*<sup>5</sup>. The *Grik1*<sup>-</sup> population was enriched for most BC  
166 and MG markers, while the *Grik1*<sup>+</sup> population was enriched for  
167 a subset of BC markers (**Supplementary Figure 2**). Accord-  
168 ingly, Gene Set Enrichment Analysis (GSEA) between *Vsx2*<sup>-</sup>  
169 and *Grik1*<sup>-</sup> populations indicated significant enrichment of rod,  
170 cone, AC, HC, and RGC markers in the *Vsx2*<sup>-</sup> populations and  
171 BC and MG markers in the *Grik1*<sup>-</sup> population (default signif-  
172 icance at FDR < 0.25; Enrichment in *Vsx2*<sup>-</sup> population: Rod:  
173 FDR < 0.001; Cone: FDR < 0.001; AC: FDR < 0.001; HC:  
174 FDR = 0.174; RGC: FDR = 0.224; Enrichment in *Grik1*<sup>-</sup> popu-  
175 lation: BC: FDR < 0.001; MG: FDR < 0.001).

176 To determine which BC subtypes were enriched in the  
177 *Grik1*<sup>-</sup> and *Grik1*<sup>+</sup> populations, we cross-referenced the DE  
178 gene set (adjusted *p*-value < 0.05) to BC subtype specific mark-  
179 ers identified by scRNA sequencing<sup>5</sup>. We found that the ma-  
180 jority of BC2, BC3A, BC3B, and BC4 markers were enriched  
181 in the *Grik1*<sup>+</sup> population as expected, and all other BC subtype  
182 markers were highly expressed in the *Grik1*<sup>-</sup> population (**Fig-**  
183 **ure 1f**). GSEA between *Grik1*<sup>-</sup> and *Grik1*<sup>+</sup> populations con-  
184 firmed these results (Enrichment in *Grik1*<sup>+</sup> population: BC2:  
185 FDR < 0.001; BC3A: FDR = 0.005; BC3B: FDR < 0.001; BC4:  
186 FDR < 0.001; Enrichment in *Grik1*<sup>-</sup> population: BC1B: FDR  
187 = 0.132; BC5A: FDR = 0.135; BC5C: FDR = 0.136; BC5D:  
188 FDR = 0.172; BC6: FDR = 0.145; BC7: FDR = 0.169; BC8/9:  
189 FDR = 0.174; RBC: FDR < 0.001). From the DE analysis, we  
190 also identified the top 20 most DE genes that were specific to a  
191 cell population (**Supplementary Figure 3**). We confirmed the  
192 expression of *Tpbgl*, a previously uncharacterized transcript, in  
193 *Grik1*<sup>+</sup> cells by SABER FISH in retinal tissue sections (**Sup-**  
194 **plementary Figure 3**). These results indicate that the cell pop-  
195 ulations isolated and profiled by Probe-Seq correspond to the  
196 expected BC subtypes.

197 We next aimed to determine the relative quality of the tran-  
198 sriptomes obtained by Probe-Seq versus those obtained from

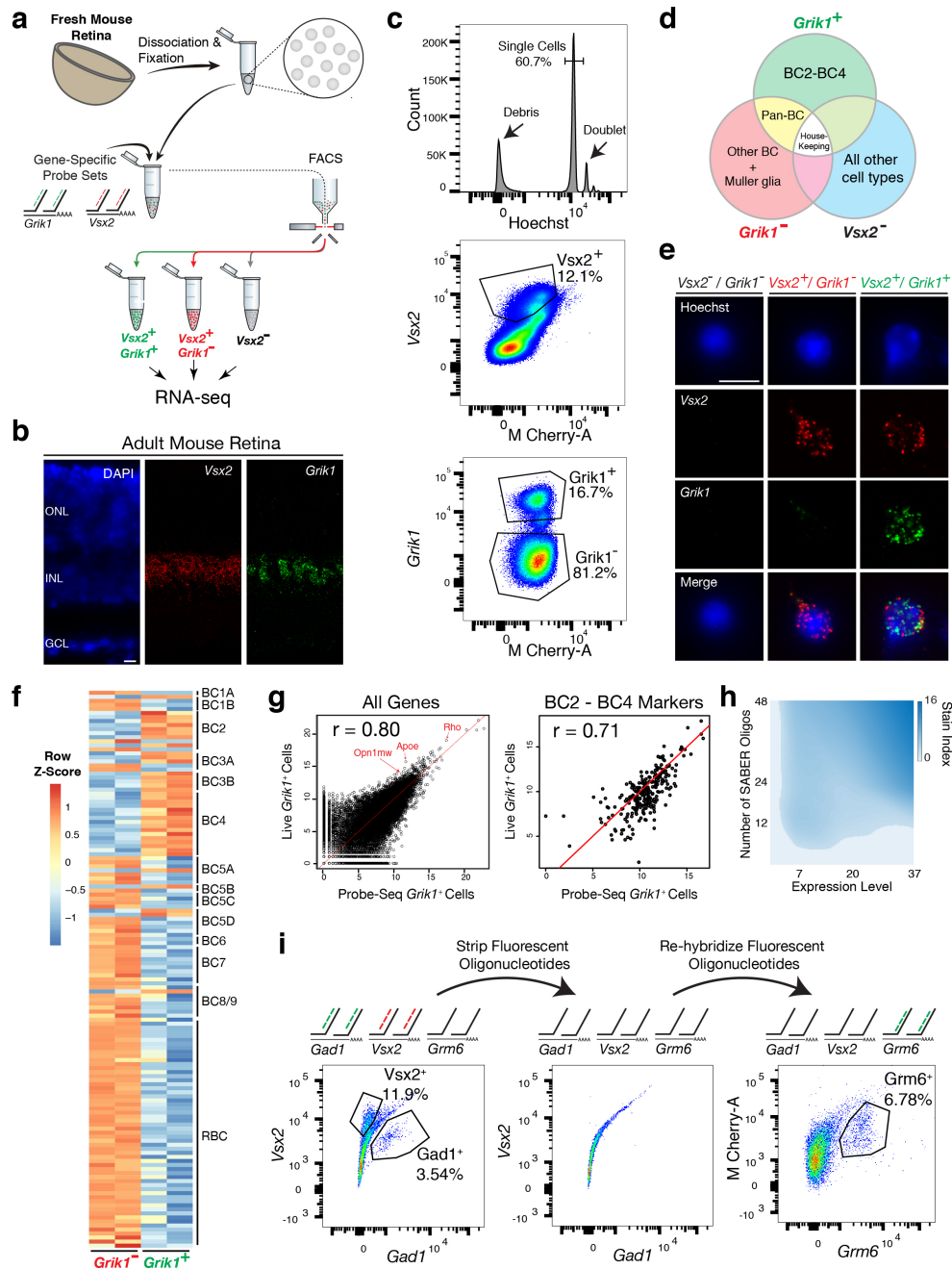


**Figure 1: Isolation and transcriptional profiling of specific BC subtypes from the adult mouse retina.** (a) Schematic of Probe-Seq for the adult mouse retina. The retina was dissociated into single cells, fixed, and permeabilized. Cells were incubated with gene-specific probe sets against *Vsx2* and *Grik1* and subsequently incubated with fluorescent oligonucleotides. Three populations of labeled cells (*Vsx2*<sup>-</sup>, *Vsx2*<sup>+</sup>/*Grik1*<sup>-</sup>, and *Vsx2*<sup>+</sup>/*Grik1*<sup>+</sup>) were isolated by FACS for downstream RNA sequencing. (b) SABER FISH signals from an adult mouse retina section using *Vsx2* and *Grik1* probe sets. (c) Representative FACS plot of all events (top panel) on a Hoechst histogram. The debris is the peak near 0. The first peak after the debris is the single cell 2N peak. 4N doublets and other cell clumps are in the peaks to the right of the single cell peak. Representative FACS plots of all single cells (middle panel) with *Vsx2* fluorescence on the y-axis and empty M-Cherry-A autofluorescence on the x-axis. The negative population ran along the diagonal. The *Vsx2*<sup>+</sup> population (12.1%) was left shifted, indicating high *Vsx2* fluorescence and low M-Cherry-A autofluorescence. FACS plot of only the *Vsx2*<sup>+</sup> population (bottom panel) with *Grik1* fluorescence on the y-axis and empty M-Cherry-A autofluorescence on the x-axis. *Vsx2*<sup>+</sup>/*Grik1*<sup>+</sup> population (16.7%) displayed strong separation from the *Vsx2*<sup>+</sup>/*Grik1*<sup>-</sup> population (81.2%). The *Grik1*<sup>MID</sup> population was included in the *Vsx2*<sup>+</sup>/*Grik1*<sup>+</sup> population. (d) Expected retinal cell type markers expressed in each isolated population. (e) Images of dissociated mouse retinal cells after the SABER FISH protocol on dissociated mouse retinal cells. (f) A heatmap representing relative expression levels of BC subtype markers previously identified by scRNA sequencing that are differentially expressed (adjusted *p*-value < 0.05) between *Grik1*<sup>-</sup> and *Grik1*<sup>+</sup> populations. (g) A representative scatter plot of log<sub>2</sub> normalized counts of all genes (left panel) or BC2-BC4 marker genes (right panel) between Live *Grik1*<sup>+</sup> cells and Probe-Seq *Grik1*<sup>+</sup> Cells. Red line indicates a slope of 1. Select cell class-specific markers (*Opn1mw*, *Apoe*, and *Rho*) are labeled in red. (h) A heatmap of the stain index with varying levels of transcript expression and number of tiling oligonucleotides. The white spaces indicate a cutoff of SI < 2. (i) Schematic and flow cytometry plots of iterative Probe-Seq. Three probe sets (*Gad1*, *Vsx2*, and *Grm6*) were hybridized to dissociated mouse retinal cells, and fluorescent oligonucleotides were hybridized only to *Gad1* and *Vsx2* probe sets to detect subsets of ACs (*Gad1*<sup>+</sup>; 3.54%) and BC/MG (*Vsx2*<sup>+</sup>; 11.9%). The fluorescent oligonucleotides were subsequently stripped with 50% formamide, which abolished the staining based on flow cytometry. Fluorescent oligonucleotides for *Grm6* were then hybridized to label a subset of BCs (*Grm6*<sup>+</sup>; 6.78%). HC, Horizontal Cell; RGC, Retinal Ganglion Cell; AC, Amacrine Cell; BC, Bipolar Cell; MG, Miller Glia; ONL, Outer Nuclear Layer; INL, Inner Nuclear Layer; GCL, Ganglion Cell Layer. Scale bars: 10 μm (b, e).



199 freshly dissociated cells. To this end, we electroporated the  
200 *Grik1*<sup>CRM4</sup>-GFP reporter plasmid into the developing retina at  
201 P2. We previously showed that 72% of GFP<sup>+</sup> cells were *Grik1*<sup>+</sup>  
202 using this reporter<sup>24</sup>. At P40, the retinas were harvested, and  
203 the electroporated region was dissociated into a single cell sus-  
204 pension. GFP<sup>+</sup> cells were FACS isolated into Trizol (henceforth  
205 called Live cells). Simultaneously, cells from the unelectropo-  
206 rated region from the same retina were used for Probe-Seq of  
207 *Grik1*<sup>+</sup> cells (henceforth called Probe-Seq cells). On average,  
208 836±155 Live cells (n=3) and 10,000±0 Probe-Seq cells (n=3),  
209 were collected for transcriptional analysis. A strong correlation  
210 of expression levels of all genes between Live and Probe-Seq  
211 cells was seen (average Pearson correlation  $r = 0.78 \pm 0.01$ ) (**Fig-**  
212 **ure 1g**). Since 72% of the GFP<sup>+</sup> population in the Live cell  
213 population were expected to be *Grik1*<sup>+</sup> cells, we expected that  
214 the correlation for markers of BC2-BC4 to be approximately  
215 0.72. Notably, when analyzing only the subtype-specific mark-  
216 ers, the correlation was 0.66 between Live and Probe-Seq cells,  
217 with enrichment of these markers in the Probe-Seq population  
218 (**Figure 1g**). Therefore, expression of GFP in *Grik1*<sup>-</sup> cells using  
219 the *Grik1*<sup>CRM4</sup>-GFP reporter plasmid could explain, at least par-  
220 tially, the discrepancy between the Probe-Seq and Live cell pop-  
221 ulations. Accordingly, DE analysis between these two popula-  
222 tions indicated enrichment of rod, cone, and MG markers, as ev-  
223 idenced by high expression of marker genes (i.e. *Rho*, *Opn1mw*,  
224 and *Apoe*) in the Live cell population (**Figure 1g**). Despite the  
225 imperfect match in the cellular compositions of these two prepa-  
226 rations, the strong correlation between the transcriptomes ob-  
227 tained by Probe-Seq and traditional live cell sorting indicates  
228 that high quality transcriptomes can be obtained by this method.

229 We next sought to investigate the parameters for SABER  
230 probe sets that are important for successful FACS isolation. We  
231 reasoned that the ability to resolve a targeted cell from the total  
232 cell population would be dependent upon the total number of fluo-  
233 rescent probes in that cell, which can be increased by targeting  
234 more tiling oligonucleotides to each transcript, or by targeting  
235 more abundant RNA species. To investigate these parameters,  
236 we generated three gene-specific probe sets, for *Grik1*, *Grm6*,  
237 and *Neto1*, which exhibit high-to-low levels of gene expres-  
238 sion based upon FISH analysis in retina tissue sections (Num-  
239 ber of puncta per positive cell: *Grik1*: 37; *Grm6*: 20; *Neto1*:  
240 6.5) (**Supplementary Figure 4**). For each gene-specific probe  
241 set, 48, 24, or 12 randomly-chosen tiling oligonucleotides were  
242 pooled for extension. These were then used for Probe-Seq, and  
243 the fluorescent signals from the FACS were analyzed to calcu-  
244 late the Stain Index (SI; see Methods for calculation of SI). This  
245 allowed for quantification of the separation of the positive pop-  
246 ulation from the negative population. The SI was found to de-  
247 crease with the reduced number of tiling oligonucleotides and  
248 the level of expression of each gene (**Figure 1h**). However,  
249 with an SI cutoff of 2, 12 tiling oligonucleotides were sufficient  
250 for confidence in the separation of gene-positive and negative  
251 populations, demonstrating that short transcripts or few tiling  
252 oligonucleotides can be used successfully for Probe-Seq.

253 To label multiple cell types, or cellular states, it is often nec-  
254 essary to use a combination of gene-specific probe sets. Ser-  
255 ial detection of markers has been achieved using SABER-FISH  
256 (Exchange-SABER). Exchange-SABER has enabled the label-

ing of seven retinal cell classes using three cycles of FISH. 257  
After each round of imaging, the fluorescent oligonucleotides 258  
are stripped using conditions that do not strip the gene-specific 259  
probe sets, allowing fluorescent channels to be reused for de- 260  
tection of different genes in the same cells. To determine 261  
whether serial multiplexing is feasible with Probe-Seq, dissoci- 262  
ated mouse retinal cells were incubated with three gene-specific 263  
probe sets for *Gad1*, *Vsx2*, and *Grm6* (**Figure 1i**). For the first 264  
round of flow cytometry, the fluorescent oligonucleotides for de- 265  
tecting *Gad1* and *Vsx2* were applied. These were assayed by 266  
flow cytometry and then stripped using 50% formamide. The 267  
removal of the fluorescent oligonucleotides was confirmed by 268  
the lack of signal in a subsequent round of flow cytometry (**Fig-** 269  
**ure 1i**). We then applied the fluorescent oligonucleotides for 270  
*Grm6* and were able to detect a new population of cells from 271  
the same cellular pool. These results indicate that serial multi- 272  
plexed Probe-Seq can allow detection of multiple cell types in 273  
the same cell preparation with iterative rounds of hybridization 274  
and FACS. 275

### 276 Probe-Seq enables isolation and RNA sequencing of cell 277 type-specific nuclei from frozen postmortem human tissue

278 To determine whether Probe-Seq will allow one to access the  
279 transcriptomes of the many archived human tissue samples, we  
280 tested the method on frozen human retinas. Nuclear prepara-  
281 tions were made, as whole cell approaches to frozen cells are  
282 not feasible<sup>30,31</sup>. The initial test was carried out on frozen mouse  
283 retinas. Nuclei were extracted by Dounce homogenization, fixed  
284 with 4% PFA, and labeled by a gene-specific probe set for *Grik1*  
285 (**Supplementary Figure 5**). *Grik1*<sup>HI</sup> (not *Grik1*<sup>MID</sup>) and *Grik1*<sup>-</sup>  
286 populations were isolated by FACS, the nuclear RNA was ex-  
287 tracted, and the cDNA was sequenced. We cross-referenced the  
288 DE gene set (adjusted  $p$ -value < 0.05) to BC subtype specific  
289 markers and found that the majority of mouse BC3A, BC3B,  
290 and BC4 markers were enriched in the *Grik1*<sup>+</sup> population, as ex-  
291 pected, and all other BC subtype markers were highly expressed  
292 in the *Grik1*<sup>-</sup> population (**Supplementary Figure 5**). These re-  
293 sults indicate that cell type-specific nuclear RNA from frozen  
294 tissue can be isolated by Probe-Seq.

295 We thus obtained fresh-frozen human retinas (age range: 40  
296 60; see Methods for full description of samples), and aimed to  
297 isolate and profile human BC subtypes using a probe set for  
298 *GRM6*, which is expressed in cone ON bipolar cells and rod  
299 bipolar cells (RBC) in the mouse and human retina<sup>5,32</sup> (**Figure**  
300 **2a**). To test the *GRM6* probe set in human retinas, it was first ap-  
301 plied to a fixed human tissue section, where signal was observed  
302 in the expected pattern, in a subset of cells in the inner nuclear  
303 layer, where BCs reside (**Figure 2b**). Nuclei were extracted  
304 from frozen human peripheral retinas, fixed, and incubated with  
305 the *GRM6* probe set. The *GRM6*<sup>-</sup> and *GRM6*<sup>+</sup> nuclei were then  
306 isolated by FACS after application of the fluorescent oligonu-  
307 cleotides (**Figure 2c**). On average, 43,000±35,500 *GRM6*<sup>-</sup> nu-  
308 clei and 1,800±781 *GRM6*<sup>+</sup> nuclei were isolated from approxi-  
309 mately 5 mm x 5 mm square of the retina per biological replicate  
310 (**Figure 2d**). SMART-Seq v.4 cDNA libraries were sequenced  
311 on NextSeq 500, with each sample sequenced to a mean depth  
312 of 18±3 million 75 bp paired-end reads. The average 3' bias for  
313 the mapped reads of the negative population was 0.70±0.04, in-  
314 dicated slight degradation of RNA. Quality control of the read



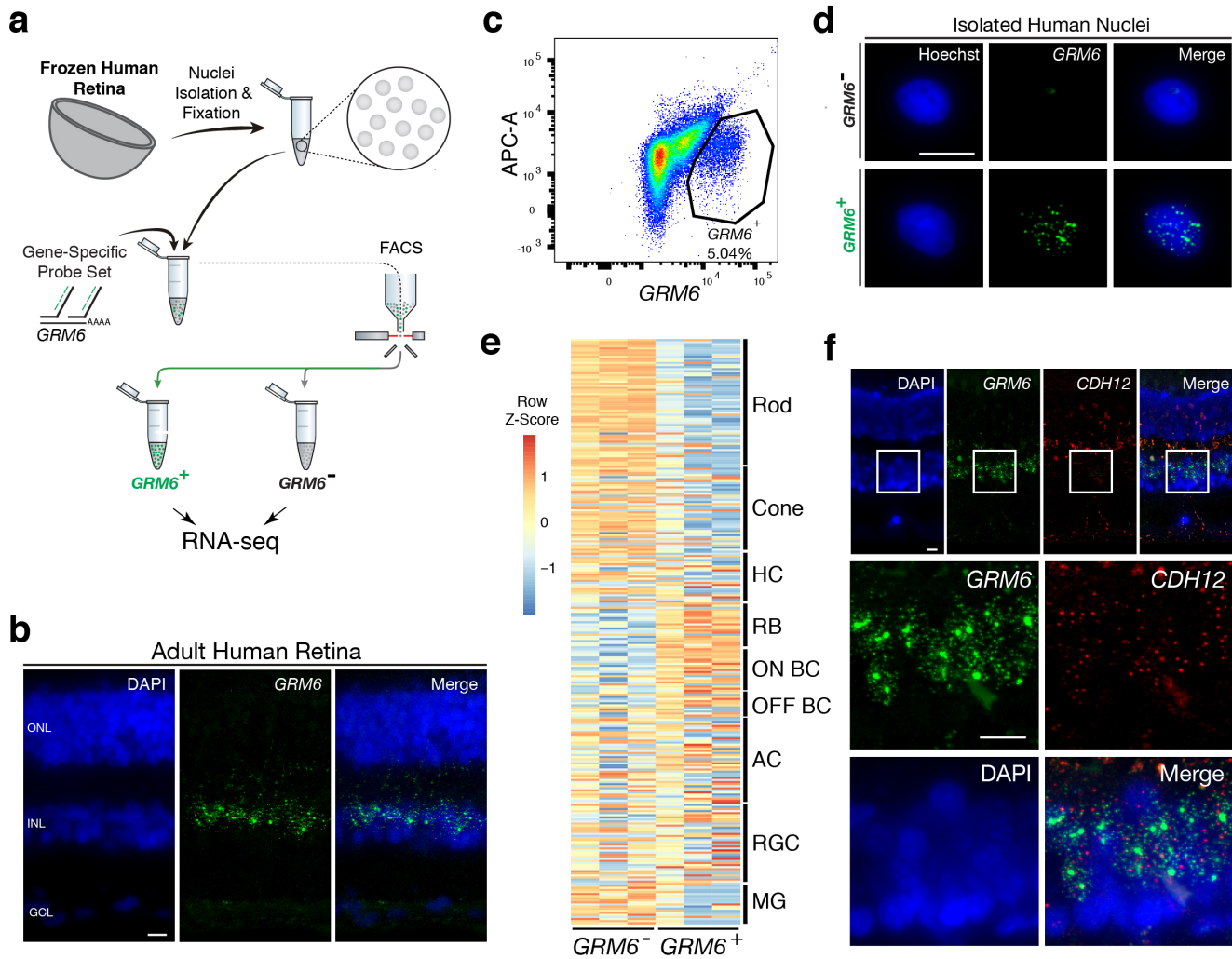


**Figure 2: Transcriptional profiling of nuclear RNA isolated from specific BC subtypes from frozen human retina.** (a) Schematic of Probe-Seq for the fresh frozen adult human retina. Single nuclei were prepared and then fixed. Nuclei were incubated with a SABER probe set for *GRM6* and then incubated with fluorescent oligonucleotides. *GRM6*<sup>+</sup> and *GRM6*<sup>-</sup> populations were isolated by FACS for downstream RNA sequencing. (b) Image of an adult human retina section probed with a SABER *GRM6* probe set. (c) FACS plot of all single nuclei with *GRM6* fluorescence on the x-axis and empty APC-A autofluorescence on the y-axis. (d) Images of isolated nuclei processed using SABER FISH for *GRM6*. (e) A heatmap representing relative expression levels of human retinal cell type markers previously identified by scRNA sequencing that are differentially expressed (adjusted *p*-value < 0.05) between *GRM6*<sup>-</sup> and *GRM6*<sup>+</sup> populations. (f) High and low magnification images of a human retinal section after the SABER FISH protocol for *CDH12*, a highly-enriched transcript in the *GRM6*<sup>+</sup> population. HC, Horizontal Cell; RGC, Retinal Ganglion Cell; AC, Amacrine Cell; ON BC, ON Bipolar Cell; RBC, Rod Bipolar Cell; OFF BC, OFF Bipolar Cell; MG, Miller Glia; ONL, Outer Nuclear Layer; INL, Inner Nuclear Layer; GCL, Ganglion Cell Layer. Scale bars: 10  $\mu$ M (b, d, f).

315 mapping and DE analysis indicated successful RNA sequencing  
 316 and DE analysis (**Supplementary Figure 6**). Upon filtering out  
 317 genes with zero counts in more than 4 samples, 1,956 out of  
 318 9,619 genes were differentially expressed (adjusted *p*-value <  
 319 0.05).

320 We compared the DE gene set (adjusted *p*-value < 0.05) to  
 321 human retinal cell type-specific markers identified by scRNA  
 322 sequencing<sup>32</sup>. We found an enrichment of markers for RBCs  
 323 and ON BCs in the *GRM6*<sup>+</sup> population (**Figure 2e**). GSEA be-  
 324 tween *GRM6*<sup>-</sup> and *GRM6*<sup>+</sup> confirmed these results (Enrichment  
 325 in *GRM6*<sup>+</sup> population: RBC: FDR = 0.003; ON BC-1: FDR =  
 326 0.181; ON BC-2: FDR = 0.126), indicating that the expected hu-  
 327 man retinal populations were accurately isolated. We validated  
 328 the expression of *CDH12*, a transcript highly enriched in the  
 329 *GRM6*<sup>+</sup> population, but previously not reported to be a marker  
 330 of these subtypes, by performing SABER FISH on fixed adult  
 331 human retina sections (**Figure 2f**). These results show that nu-  
 332 clear transcripts isolated from frozen tissue by Probe-Seq are

sufficient for transcriptional profiling.

### Isolation and transcriptional profiling of intestinal stem cells from the *Drosophila* midgut

To determine whether Probe-Seq can be successfully applied to non-CNS cells, and to cells from invertebrates, we applied the method to the midgut of *Drosophila melanogaster*. The adult *Drosophila* midgut is composed of four major cell types - enterocytes (EC), enteroendocrine cells (EE), enteroblasts (EB), and intestinal stem cells (ISC), though recent profiling studies have revealed heterogeneity among ECs and ISC/EBs<sup>33,34</sup>. We aimed to isolate ISCs and EBs using a gene-specific probe set for escargot (*esg*), a well-characterized marker for these cell types (**Figure 3a**). As SABER-FISH had not yet been tested on *Drosophila* tissue, we first tested this method on wholemounts of the *Drosophila* gut. SABER FISH signal was observed in the appropriate pattern, in a subset of midgut cells (**Figure 3b**). To perform Probe-Seq, we dissociated 35-40 *Drosophila* midguts

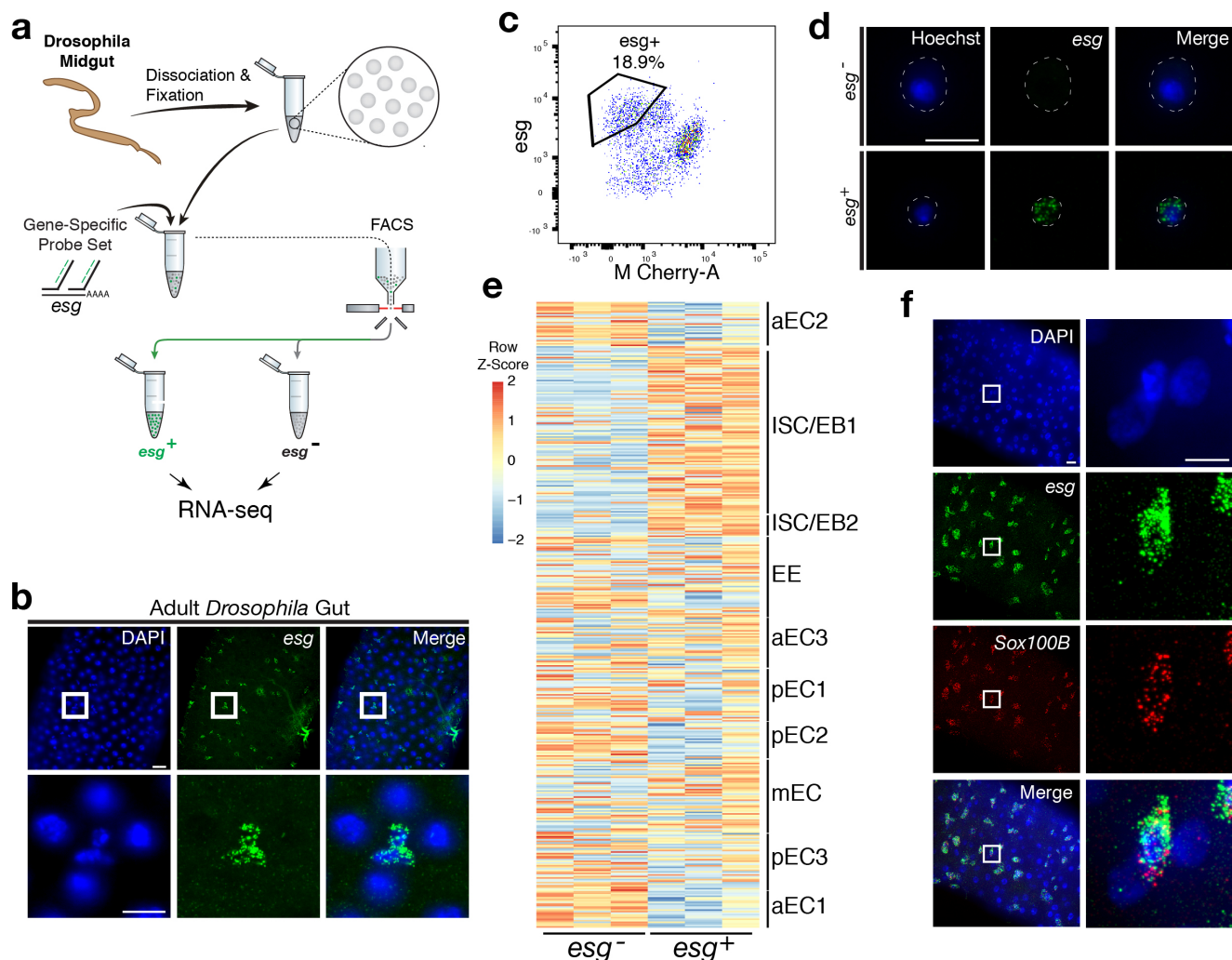


**Figure 3: Isolation and transcriptional profiling of ISC/EBs from the adult *Drosophila* midgut.** (a) Schematic of Probe-Seq for the adult *Drosophila* midgut. Midguts from 7-10-day old female flies were dissociated into single cells and fixed. Cells were incubated with a SABER FISH probe set for *esg* and subsequently incubated with fluorescent oligonucleotides. *esg*<sup>+</sup> and *esg*<sup>-</sup> populations were isolated by FACS for downstream RNA sequencing. (b) Image of a wholemount adult *Drosophila* midgut following the SABER FISH protocol using an *esg* probe set. (c) FACS plot of all single cells with *esg* fluorescence on the y-axis and empty M-Cherry-A autofluorescence on the x-axis. (d) Images of isolated midgut cells processed using SABER FISH for *esg*. The white dotted lines demarcate cell outlines. (e) A heatmap representing relative expression levels of differentially expressed (adjusted *p*-value < 0.05) genes for *Drosophila* gut cell type markers previously identified by scRNA sequencing, between *esg*<sup>-</sup> and *esg*<sup>+</sup> populations. (f) Images of a *Drosophila* midgut wholemount after the SABER FISH protocol for an ISC/EB marker, *Sox100B*, a highly-enriched transcript in the *esg*<sup>+</sup> population. EC, Enterocyte; ISC, Intestinal Stem Cell; EB, Enteroblast; EE, Enteroendocrine Cell. Scale bars: 10  $\mu$ M (d, f, right panels); 20  $\mu$ M (b, upper panels f, left panels).

per biological replicate, fixed in 4% PFA, and incubated the cells with the *esg* probe set. FACS was then used to sort *esg*<sup>-</sup> and *esg*<sup>+</sup> populations (Figure 3c-d). As only the 2N single cells were sorted, proliferating ISCs and polyploid ECs were excluded. On average, 1,400±208 *esg*<sup>-</sup> cells and 1,000±404 *esg*<sup>+</sup> cells per biological replicate were isolated. SMART-Seq v.4 cDNA libraries were sequenced on NextSeq 500 to a mean of 16±4 million 75 bp paired-end reads. Quality control of the read mapping and DE analysis indicated successful RNA sequencing and DE analysis (Supplementary Figure 7). Upon filtering out genes with zero counts in more than 3 samples, 405 out of 1,596 genes were differentially expressed (adjusted *p*-value < 0.05).

The DE gene set (adjusted *p*-value < 0.05) from Probe-Seq was compared to cell type-specific markers identified by scRNA sequencing<sup>34</sup>. An enrichment of ISC/EB1 and ISC/EB2 markers was observed in the *esg*<sup>+</sup> population isolated using Probe-Seq, while markers of all other cell types were enriched in the *esg*<sup>-</sup> population (Figure 3e). GSEA between *esg*<sup>+</sup> and *esg*<sup>-</sup> popula-

tions isolated using Probe-Seq indicated significant enrichment of ISC/EB1 and ISC/EB2 markers in the *esg*<sup>+</sup> population and all other cell type markers in the *esg*<sup>-</sup> population (Enrichment in *esg*<sup>+</sup> population: ISC/EB1: FDR < 0.001; ISC/EB2: FDR = 0.081; Enrichment in *esg*<sup>-</sup> population: aEC1: FDR < 0.001; aEC2: FDR < 0.001; pEC2 FDR < 0.001; pEC1: FDR < 0.001; pEC3: FDR < 0.001; EE: FDR < 0.001; aEC3: FDR = 0.009; mEC: FDR = 0.041). Using SABER FISH on wholemounts of midguts, we validated the co-localization of *esg* and *Sox100B*, a transcript significantly enriched in the *esg*<sup>+</sup> population (Figure 3f). Additionally, we cross-referenced the Probe-Seq DE gene set (adjusted *p*-value < 0.05) to ISC/EB and EC markers defined by DamID profiling of the adult *Drosophila* gut<sup>35</sup>. From this analysis, the majority of ISC/EB and EC markers were seen to be enriched in *esg*<sup>+</sup> and *esg*<sup>-</sup> populations, respectively (Supplementary Figure 8). These results demonstrate that Probe-Seq enables the isolation and transcriptional profiling of specific cell types from invertebrate non-CNS tissue.

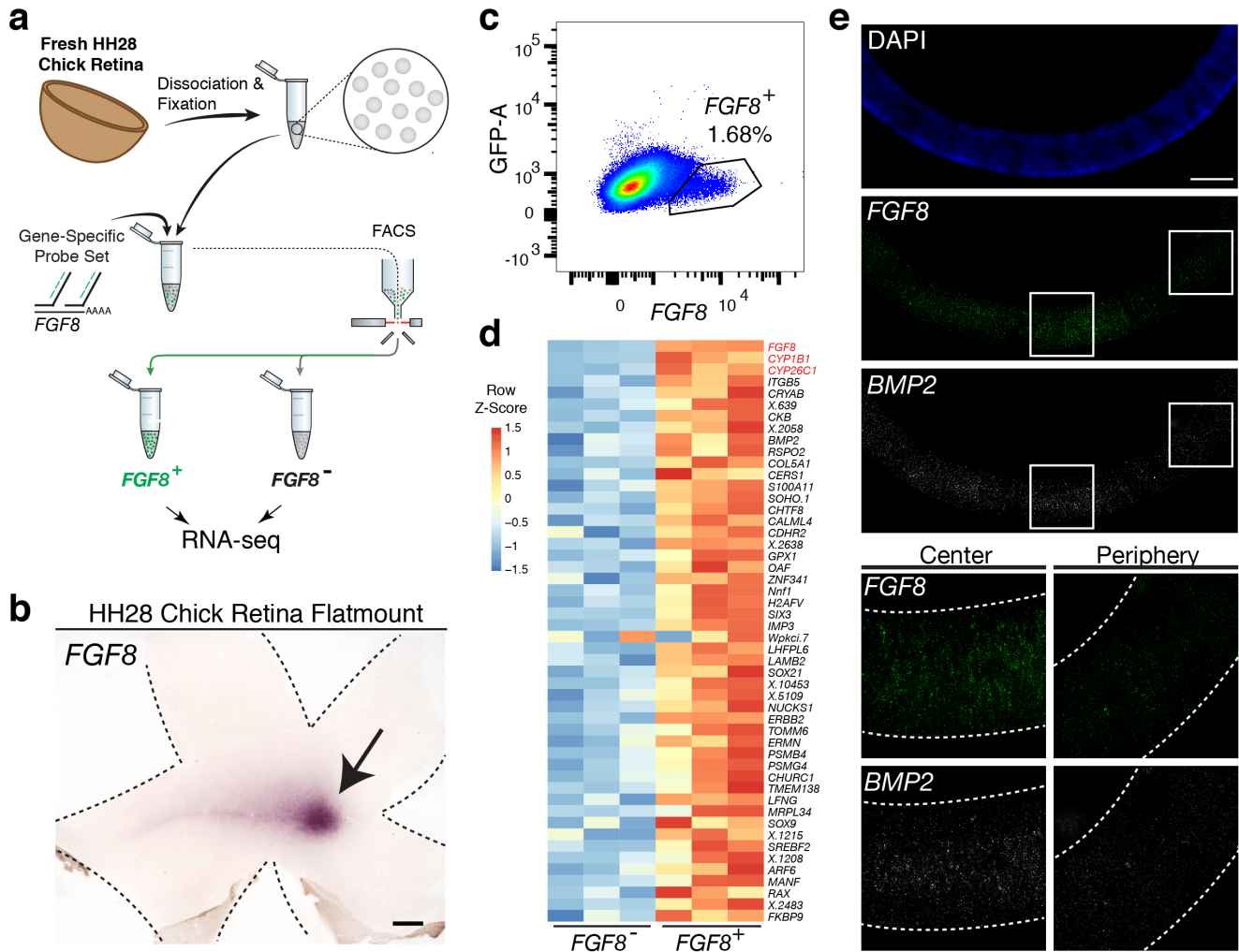


**Figure 4: Probe-Seq identifies the transcriptional landscape of chick central progenitor cells that give rise to the high acuity area.** (a) Schematic of Probe-Seq for the developing HH28 chick retina. The chick retina was dissociated into single cells and fixed. Cells were incubated with a SABER FISH probe set for *FGF8* and subsequently incubated with fluorescent oligonucleotides. *FGF8*<sup>+</sup> and *FGF8*<sup>-</sup> populations were isolated by FACS for downstream RNA sequencing. (b) FACS plot of all single cells with *FGF8* fluorescence on the x-axis and empty GFP-A autofluorescence on the y-axis. (c) A heatmap of unbiased top 50 genes that were enriched in the *FGF8*<sup>+</sup> population compared to the *FGF8*<sup>-</sup> population. (d) Images of a section spanning the central HH28 chick retina after the SABER FISH protocol for *FGF8* and *BMP2*, a transcript highly enriched in the *FGF8*<sup>+</sup> population. Scale bars: 500  $\mu$ M (b); 50  $\mu$ M (e).

### 386 Transcriptome profiling of the central chick retina reveals 387 unique transcripts expressed in cells that give rise to the high 388 acuity area

389 The central chicken retina contains a region thought to endow  
390 high acuity vision, given its cellular composition and arrange-  
391 ment of cells. It comprises a small and discrete area that is de-  
392 void of rod photoreceptors and enriched in cone photoreceptors,  
393 with a high density of retinal ganglion cells, the output neurons  
394 of the retina<sup>36,37</sup>. These features are shared with the high acuity  
395 areas (HAA) of other species, including human. Although  
396 we have shown that *FGF8*, *CYP26C1*, and *CYP26A1* are highly  
397 enriched in this area at embryonic day 6 (E6)<sup>37</sup>, the other molec-  
398 ular determinants that may play a role in HAA development  
399 are unknown. Probe-Seq was thus used to isolate and sequence  
400 *FGF8*<sup>+</sup> cells. Hamburger-Hamilton stage 28 (HH28) chick reti-  
401 nas were dissociated into single cells, fixed, and probed for the  
402 *FGF8* transcript (Figure 4a). On average,  $7,000 \pm 6,950$  *FGF8*<sup>+</sup>  
403 cells and  $189,000 \pm 19,000$  *FGF8*<sup>-</sup> cells were FACS isolated into  
404 individual populations (Figure 4b). The cDNA from each popu-  
405 lation (n=3) was sequenced to a mean depth of  $18 \pm 7$  million

75bp paired-end reads on NextSeq 500. Interestingly, the 3' bias  
of the mapped reads from the chick retina was significantly re-  
duced compared to that of the mouse retina ( $0.59 \pm 0.04$ , compa-  
rable to RIN 6-8) (Supplementary Figure 9). Quality control  
of the read mapping and DE analysis indicated successful RNA  
sequencing and DE analysis (Supplementary Figure 10). Be-  
tween *FGF8*<sup>-</sup> and *FGF8*<sup>+</sup> populations, we found 1,924 DE genes  
out of 12,053 genes.

Among the top 50 most enriched DE transcripts in the  
*FGF8*<sup>+</sup> population were *FGF8*, *CYP1B1*, and *CYP26C1* (Fig-  
ure 4c). The latter two transcripts are components of the retinoic  
acid signaling pathway, and were previously shown to be highly  
enriched in the central retina where *FGF8* is expressed<sup>37</sup>. Pre-  
viously, *FGF8* expression was shown to be largely confined to  
the area where progenitor cells reside. However, it was unclear  
whether it was also expressed in differentiated cells<sup>37</sup>. DE anal-  
ysis of the *FGF8*<sup>-</sup> and *FGF8*<sup>+</sup> populations revealed enrichment  
of early differentiation markers of RGCs (i.e. *NEFL*) and pho-  
toreceptors (i.e. *NEUROD1*) in the *FGF8*<sup>-</sup> population, confirm-  
ing that *FGF8* is mostly expressed in central progenitor cells



(Supplementary Figure 11). As we wished to validate the DE genes using FISH on sections, and SABER FISH had not yet been tested on chick tissue, we first tested the method using the *FGF8* probe set on chick tissue sections (Figure 4e). Robust and specific FISH signal was seen in the appropriate pattern for *FGF8*. An additional SABER-FISH probe set for *BMP2*, a transcript enriched in the *FGF8*<sup>+</sup> population, was then used on developing HH28 chick central retinal sections. *BMP2* was found to be highly enriched within the *FGF8*<sup>+</sup> population, i.e expression was confined to a discrete central retina where *FGF8* was expressed (Figure 4e). These results indicate that Probe-Seq of the developing chick retina using *FGF8* as a molecular handle can reveal the transcriptional profile of the progenitor cells that will comprise the chick high acuity area.

## DISCUSSION

Studies of model organisms have allowed the dissection of molecular mechanisms that underlie a variety of biological processes. However, each organism across the evolutionary tree possesses unique traits, and understanding these traits will greatly enrich our understanding of biological processes. Non-model organisms can now be investigated at the genetic level, due to advances in DNA sequencing, transcriptional profiling, and genome modification methods. Despite progress, challenges remain to achieve greater depth in the characterization of the transcriptomes of rarer cell types within heterogeneous tissues. Even in model organisms, deep transcriptional profiling of specific cell types remains difficult if specific cis-regulatory elements are unavailable. To overcome these challenges, we developed Probe-Seq.

Probe-Seq uses a FISH method based upon SABER probes to hybridize gene-specific probe sets to RNAs of interest<sup>24</sup>. This method provides amplified fluorescent detection of RNA molecules and can be spectrally or serially multiplexed to mark cell populations based on combinatorial RNA expression profiles. Previously-identified markers can thus be targeted by gene-specific probe sets to isolate specific cell types by FACS. Subsequently, deep RNA sequencing can be carried out on the sorted population to generate cell type-specific transcriptome profiles. Due to the reliance on RNA for cell sorting, rather than protein, this method is applicable across organisms. Other RNA-based methods to label specific cell types for downstream sequencing have not been tested with tissue samples, and/or require cell encapsulation in a microfluidic device<sup>25,38,39</sup>.

Probe-Seq allowed the isolation and profiling of RNA from fresh mouse, frozen human, and fresh chick retinas, as well as gut cells from *Drosophila melanogaster*. Aside from the different dissociation protocols, Probe-Seq does not require species- or tissue-specific alterations. To profile multiple cellular subtypes, serial multiplexed Probe-Seq allows for iterative labeling, sorting, and re-labeling. This strategy enables separation of FACS-isolated, broad populations into finer sub-populations. The Probe-Seq method is also cost and time effective, with less than 6 hours of hands-on time, including FISH, FACS, and library preparation. Per sample, we estimate the cost to be less than \$200, from start to finish, achieving 15 million paired-end reads. The Probe-Seq protocol may be further optimized to maximize utility. For example, the protocol may be fur-

ther modified to use other single molecule FISH methods such as clampFISH<sup>40</sup> or RNAscope<sup>41</sup> rather than SABER-FISH, as these methods have their respective strengths and weaknesses. Additionally, the protocol may also be adapted to use a cell strainer for the wash steps to minimize cell loss from centrifugation. Further development for scRNA sequencing after cell type enrichment using Probe-Seq may also be possible. For this, however, adaptation of Probe-Seq for the reversal of crosslinks for scRNA sequencing<sup>42-44</sup> will likely be necessary.

## METHODS

### Mouse retina samples

All animals were handled according to protocols approved by the Institutional Animal Care and Use Committee (IACUC) of Harvard University. For fresh samples, retinas of adult CD1 mice (>P30) from Charles River Laboratories were dissected. For frozen samples, retinas of adult CD1 mice (>P30) were dissected and frozen in a slurry of isopentane and dry ice and kept at -80°C.

### Human retina samples

Frozen eyes were obtained from Restore Life USA (Elizabethton, TN) through TissueForResearch. Patient DRLU041818C was a 53-year-old female with no clinical eye diagnosis and the postmortem interval was 9 hours. Patient DRLU051918A was a 43-year-old female with no clinical eye diagnosis and the postmortem interval was 5 hours. Patient DRLU031318A was a 47-year-old female with no clinical eye diagnosis and the postmortem interval was 7 hours. This IRB protocol (IRB17-1781) was determined to be not-human subject research by the Harvard University-Area Committee on the Use of Human Subjects.

### Chick retina samples

Fertilized White Leghorn eggs from Charles River Laboratories were incubated at 38°C with 40% humidity. Embryos were staged according to Hamburger and Hamilton up to HH28<sup>45</sup>.

### *Drosophila melanogaster* midgut samples

Tissues were dissected from female 7-10-day-old adult Oregon-R *Drosophila melanogaster*. Flies were reared on standard cornmeal/agar medium in 12:12 light:dark cycles at 25°C.

### Dissociation of mouse and chick retinas

Mouse or chick retinas were dissected away from other ocular tissues in Hanks Balanced Salt Solution (Thermo Fisher Scientific, cat. #14025092) or PBS. The retina was then transferred to a microcentrifuge tube and incubated for 7 minutes at 37°C with an activated papain dissociation solution (87.5 mM HEPES pH 7.0 (Thermo Fisher Scientific, cat. #15630080), 2.5 mM L-Cysteine (MilliporeSigma, cat. #168149), 0.5 mM EDTA pH 8.0 (Thermo Fisher Scientific, cat. #AM9260G), 10  $\mu$ L Papain Suspension (Worthington, cat. #LS0003126), 19.6  $\mu$ L UltraPure Nuclease-Free Water (Thermo Fisher Scientific, cat. #10977023), HBSS up to 400  $\mu$ L, activated by a 15-minute incubation at 37°C). The retina was then centrifuged at 600 xg for 3 minutes. The supernatant was removed, and 1 mL of HBSS/10% FBS (Thermo Fisher Scientific, cat. #10437028) was added without agitation to the pellet. The pellet was centrifuged at 600 xg for 3 minutes. The supernatant was removed, and 600  $\mu$ L of trituration buffer (DMEM (Thermo Fisher Scientific, cat. #11995065), 0.4% (wt/vol) Bovine Serum Albumin (MilliporeSigma cat. #A9418)) was added. The pellet was dissociated by trituration at room temperature (RT) using a P1000 pipette up to 20 times or until the solution was homogenous.

### Dissociation of *Drosophila* midgut

35-40 *Drosophila* midguts were dissected in PBS and transferred to 1% BSA/PBS solution. The midguts were incubated in 400  $\mu$ L of Elastase/PBS solution (1 mg/mL, MilliporeSigma cat. #E0258) for 30 minutes to 1 hour at RT, with trituration with a P1000 pipette every 15 minutes. 1 mL of 1% BSA/PBS was then added. This solution was overlaid on top of Optiprep/PBS (MilliporeSigma, cat. #D1556) solution with a density of 1.12 g/mL in a 5-mL polypropylene tube (Thermo Fisher Scientific, cat. #1495911A). The solution was centrifuged at 800 xg at RT for 20 minutes. The top layer with viable cells was collected for further processing.

### Mouse and human frozen nuclei isolation

Upon thawing, tissue was immediately incubated in 1% PFA (with 1  $\mu$ L mL<sup>-1</sup> RNasin Plus (Promega, cat. #N2611)) for 5 minutes at 4°C. Nuclei were pre-

pared by Dounce homogenizing in Homogenization Buffer (250 mM sucrose, 25 mM KCl, 5 mM MgCl<sub>2</sub>, 10mM Tris buffer, pH 8.0, 1 μM DTT, 1x Protease Inhibitor (Promega, cat. #6521), Hoechst 33342 10 ng mL<sup>-1</sup> (Thermo Fisher Scientific, cat. #H3570), 0.1% Triton X-100, 1 μL mL<sup>-1</sup> RNasin Plus). Sample was then overlaid on top of 20% sucrose solution (25 mM KCl, 5 mM MgCl<sub>2</sub>, 10mM Tris buffer, pH 8.0) and spun at 500 xg for 12 minutes at 4°C.

#### 554 Probe-Seq for whole cells and nuclei

555 For all solutions, 1 μL mL<sup>-1</sup> RNasin Plus was added 10 minutes before use. If  
556 the cells or nuclei were not already pelleted, the suspended cells/nuclei (hence-  
557 forth called cells) were centrifuged at 600 xg for 5 minutes at 4°C. The cells  
558 were then resuspended in 1 mL of 4% PFA (Electron Microscopy Sciences, cat.  
559 #15714S, diluted in PBS) and incubated at 4°C for 15 minutes with rocking.  
560 The cells were centrifuged at 2000 xg for 5 minutes at 4°C. Except in the case  
561 of nuclei, the supernatant was removed, and the cells were resuspended in 1 mL  
562 of Permeabilization Buffer (Hoechst 33342 10 μg mL<sup>-1</sup>, 0.1% Triton X-100,  
563 PBS up to 1 mL) and incubated for 10 minutes at 4°C with rocking. For both  
564 cells and nuclei, the cells were next centrifuged at 2000 xg for 5 minutes at 4°C.  
565 The supernatant was removed, and the cells were resuspended in 500 μL of  
566 pre-warmed (43°C) 40% wash Hybridization solution (wHyb; 2x SSC (Thermo  
567 Fisher Scientific, cat. #15557044), 40% deionized formamide (MilliporeSigma,  
568 cat. #S4117), diluted in UltraPure Water). Compared to the original SABER  
569 protocol<sup>24</sup>, the Tween-20 was removed as we found that it causes cell clumping.  
570 The cells were incubated for at least 30 minutes at 43°C. After this step, the cell  
571 pellet became transparent. The cells were centrifuged at 2000 xg for 5 minutes  
572 at RT, and the supernatant was carefully removed, leaving ~100 μL of super-  
573 natant. The cells were then resuspended in 100 μL of pre-warmed (43°C) Probe  
574 Mix (1 μg of probe per gene, 96 μL of Hyb1 solution (2.5x SSC, 50% deion-  
575 ized formamide, 12.5% Dextran Sulfate (MilliporeSigma cat. #D8906)), diluted  
576 up to 120 μL with UltraPure Water) and incubated overnight (16-24 hours) at  
577 43°C.

578 500 μL of pre-warmed (43°C) 40% wHyb was added to the cells and centri-  
579 fugged at 2000 xg for 5 minutes at RT. The supernatant was removed, and the  
580 cells were resuspended in 500 μL of pre-warmed (43°C) 40% wHyb. The cells  
581 were incubated for 15 minutes at 43°C. The cells were then centrifuged at 2000  
582 xg for 5 minutes at RT, and the supernatant was removed. 1 mL of pre-warmed  
583 (43°C) 2x SSC solution was added, the cells were resuspended, and incubated  
584 for 5 minutes at 43°C. The cells were centrifuged at 2000 xg for 5 minutes at  
585 RT, and the supernatant was removed. Cells were then resuspended in 500 μL of  
586 pre-warmed (37°C) PBS. The cells were centrifuged at 2000 xg for 5 minutes at  
587 RT, and the supernatant was removed. The cells were resuspended in 100 μL of  
588 Fluorescent Oligonucleotide Mix (100 μL of PBS, 2 μL of each 10 μM Fluores-  
589 cent Oligonucleotide) and incubated for 10 minutes at 37°C. After incubation,  
590 500 μL of pre-warmed (37°C) PBS was added and the cells were centrifuged at  
591 2000 xg for 5 minutes at RT. The supernatant was removed, and the cells were  
592 resuspended in 500 μL of pre-warmed (37°C) PBS. The cells were incubated  
593 for 5 minutes at 37°C. The cells were centrifuged at 2000 xg for 5 minutes at  
594 RT, the supernatant was removed, and the cells were resuspended in 500-1000  
595 μL of PBS, depending on cell concentration.

#### 596 FACS isolation of specific cell types

597 The suspended labeled cells were kept on ice before FACS. Immediately before  
598 FACS, the cells were filtered through a 35 μM filter (Thermo Fisher Scientific,  
599 cat. #352235) for mouse, chick, and human retina cells/nuclei or a 70 μM filter  
600 (Thermo Fisher Scientific, cat. #352350) for *Drosophila* cells. FACSAria (BD  
601 Biosciences) with 488, 561, 594, and 633 lasers was used for the sorts. 2N sin-  
602 gle cells were gated based on the Hoechst histogram. For the *Drosophila* gut,  
603 debris was gated out first by FSC/SSC plot because the high number of debris  
604 events masked the Hoechst<sup>+</sup> peaks. Out of the single cells, a 2-dimensional plot  
605 (with one axis being the fluorescent channel of interest and another axis that is  
606 empty) was used to plot the negative and positive populations. The events that  
607 ran along the diagonal in this plot were considered negative, and the positive  
608 events were either left- or right-shifted (depending on axes) compared to the di-  
609 agonal events. For some samples, the number of sorted cells was capped, as  
610 indicated by a standard deviation of 0. Different populations were sorted into  
611 microcentrifuge tubes with 500 μL of PBS and kept on ice after FACS. The pro-  
612 tocol was later modified so that the cells are sorted into 500 μL of 1% BSA/PBS,  
613 as this significantly improved cell pelleting. The data obtained for this study did  
614 not use 1% BSA/PBS.

#### 615 RNA isolation and library preparation

616 The sorted cells were transferred to a 5-mL polypropylene tube and centrifuged  
617 at 3000 xg for 7 minutes at RT. The supernatant was removed as much as possi-  
618 ble, the cells were resuspended in 100 μL Digestion Mix (RecoverAll Total  
619 Nuclear Isolation Kit (Thermo Fisher Scientific, cat. #AM1975) 100 μL of Di-

gestion Buffer, 4 μL of protease), and incubated for 3 hours at 50°C, which  
differs from the manufacturer's protocol. The downstream steps were accord-  
ing to the manufacturer's protocol. The volume of ethanol/additive mix in the  
kit was adjusted based on the total volume (100 μL of Digestion Mix and re-  
maining volume after cell pelleting). The libraries for RNA sequencing were  
generated using the SMART-Seq v.4 Ultra Low Input RNA kit (Takara Bio, cat.  
#634890) and Nextera XT DNA Library Prep Kit (Illumina, cat. #FC1311096)  
according to the manufacturer's protocol. The number of cycles for SMART-  
Seq v.4 protocol was as follows: Mouse *Vsx2/Grik1*: 13 cycles; Chick *FGF8*:  
16 cycles; Human *GRM6*: 16 cycles; *Drosophila esg*: 17 cycles. 150 pg of total  
cDNA was used as the input for Nextera XT after SMART-Seq v.4, and 12 cycles  
were used except for *Drosophila* samples for which 14 cycles were necessary.  
The cDNA library fragment size was determined by the BioAnalyzer 2100 HS  
DNA Assay (Agilent, cat. #50674626). The libraries were sequenced as 75bp  
paired-end reads on NextSeq 500 (Illumina).

#### 635 RNA-Seq data analysis

636 Quality control of RNA-seq reads were performed using fastqc version  
637 0.10.1 (<https://www.bioinformatics.babraham.ac.uk/projects/fastqc/>). RNA-seq  
638 reads were clipped and mapped onto the either the mouse genome (En-  
639 sembl GRCm38.90), human genome (Ensembl GRCh38.94), chick genome  
640 (Ensembl GRCg6a.96), or *Drosophila* genome (BDGP6.22) using STAR  
641 version 2.5.2b<sup>46,47</sup>. Parameters used were as follows: `-runThreadN`  
642 `6 -readFilesCommand zcat -outSAMtype BAM SortedByCoordinate -`  
643 `outSAMunmapped Within -outSAMattributes Standard -clip3pAdapterSeq -`  
644 `quantMode TranscriptomeSAM GeneCounts`

645 Alignment quality control was performed using Qualimap version 2.2.1<sup>48</sup>.  
646 Read counts were produced by HT-seq version 0.9.1<sup>49</sup>. Parameters used were as  
647 follows: `-i gene.name -s no`

648 The resulting matrix of read counts were analyzed for differential expres-  
649 sion by DESeq2 version 3.9<sup>50</sup>. For the DE analysis of human and *Drosophila*  
650 samples, any genes with more than 4 and 3 samples with zero reads, respec-  
651 tively, were discarded. The R scripts used for differential expression analysis  
652 are available in Supplementary Files.

#### 653 Gene set curation

654 Unique marker genes that define different cell types in different tissue types  
655 were curated in an unbiased manner. For the mouse retina, marker genes of  
656 major cell types were identified from scRNA sequencing<sup>3</sup>. Genes that were  
657 found in more than one cluster were removed from the analysis to obtain unique  
658 cluster-specific markers. Rod-specific genes were highly represented in all clus-  
659 ters; thus, they were considered non-unique by this analysis. Therefore, top 20  
660 rod-specific genes were manually added after non-unique genes were removed.  
661 For mouse BCs, marker genes of BC subtypes with high confidence were iden-  
662 tified by scRNA sequencing<sup>5</sup>. Genes that were found in more than one cluster  
663 were removed from the analysis. For the human retina, marker genes of major  
664 cell types were identified by scRNA sequencing<sup>32</sup>. Marker genes that were ex-  
665 pressed in < 90% of cells in the cluster were removed for analysis. For the  
666 *Drosophila* gut, marker genes of major cell types were identified from DamID  
667 transcriptional profiling and scRNA sequencing<sup>34,35</sup>. For the DamID dataset, a  
668 cutoff of FDR < 0.01 was used for marker genes that were specifically expressed  
669 between ISC/EBs and ECs.

#### 670 Gene set enrichment analysis

671 GSEAPreranked analysis was performed using GSEA v3.0<sup>51</sup>. Curated gene sets  
672 described above were used to define various cell types. Parameters used were  
673 as follows: Number of permutations: 1000; Enrichment statistic: classic; the  
674 ranked file was generated using log<sub>2</sub>FoldChange generated by DESeq2. To de-  
675 termine significance, we used the default FDR < 0.25 for all gene sets.

#### 676 SABER probe synthesis

677 SABER probe sets were synthesized using the original protocol<sup>24</sup>. The gene  
678 of interest was searched in the UCSC Genome Browser. Then, the BED  
679 files for genes of interest were generated through the UCSC Table Browser  
680 with the following parameters: group: Genes and Gene Predictions; track:  
681 NCBI RefSeq; table: UCSC RefSeq (refGene); region: position; output for-  
682 mat: BED; Create one BED record per: Exons. If multiple isoforms were  
683 present in the BED output file, all but one was removed manually. Genome-  
684 wide probe sets for mouse, human, chick, and *Drosophila* were downloaded  
685 from (<https://oligopaints.hms.harvard.edu/genome-files>) with Balance setting.  
686 The tiling oligonucleotide sequences were generated using intersectBed (bed-  
687 tools 2.27.1) between the BED output file and the genome-wide chromosome-  
688 specific BED file with f 1. If the BED file sequences were on the + strand, the  
689 reverse complement probe set was generated using OligoMiners probeRC.py  
690 script (<https://github.com/brianbeliveau/OligoMiner>). For each tiling oligonu-  
691 cleotide sequence, hairpin primer sequences were added following a TTT linker.



692 The tiling oligonucleotides were ordered from IDT with the following speci- 764  
693 fications in a 96-well format: 10 nmole, resuspended in IDTE pH 7.5, V-Bottom 765  
694 Plate, and normalized to 80  $\mu$ M. The tiling oligonucleotides were then com- 766  
695 bined into one pool for gene-specific probe set synthesis using a multi-channel 767  
696 pipette. The tiling oligonucleotide sequences for every gene-specific probe set 768  
697 used in this study are provided in Supplementary Files. 769

698 Tiling oligonucleotides were extended by a PER concatemerization reaction 770  
699 (1X PBS, 10 mM MgSO<sub>4</sub>, dNTP (0.3 mM of A, C, and T), 0.1  $\mu$ M Clean.G, 0.5 771  
700  $\mu$ L Bst Polymerase (McLab, cat. #BPL-300), 0.5  $\mu$ M hairpin, 1  $\mu$ M oligonu- 772  
701 cleotide pool). The reaction was incubated without the tiling oligonucleotide 773  
702 pool for 15 minutes at 37°C. Then, the oligonucleotide pool was added and the 774  
703 reaction was incubated for 100 minutes at 37°C, 20 minutes at 80°C, and in- 775  
704 cubated at 4°C until probe set purification. 8  $\mu$ L of the reaction was analyzed 776  
705 on an 1.25% agarose gel (run time of 8 minutes at 150 volts) to confirm the 777  
706 probe set length. Probe sets of 300-700 nt were used for the study. The 37°C 778  
707 extension time was increased or decreased (from 100 minutes) based on desired 779  
708 concatemer length. The probe set was purified using MinElute PCR Purification 780  
709 Kit (Qiagen, cat. #28004) following manufacturers protocol. The probe set was 781  
710 eluted in 25  $\mu$ L UltraPure Water and the concentration was analyzed by Nano- 782  
711 Drop on the ssDNA setting (Thermo Fisher Scientific). Probe sets with ssDNA 783  
712 concentration ranging from 200-500 ng/ $\mu$ L, depending on the hairpin, were used 784  
713 for this study. 785

714 Fluorescent oligonucleotides were ordered from IDT with 5' modification 786  
715 of either AlexaFluor 488, ATTO 550, ATTO 590, or ATTO 633. The sequences 787  
716 for fluorescent oligonucleotides and hairpins are included in Supplementary 788  
717 Files. Working dilutions of the hairpins (5  $\mu$ M) and tiling oligonucleotides (10 789  
718  $\mu$ M) were made by diluting in IDTE pH 7.5 and stored at -20°C. Working di- 790  
719 lutions of the fluorescent oligonucleotides (10  $\mu$ M) were made by diluting in 791  
720 UltraPure Water and stored at -20°C. 792

#### 721 **Fluorescent oligonucleotide stripping for multiplexed Probe-Seq**

722 Cells were incubated in 50% formamide solution (diluted in PBS) for 5 minutes 793  
723 at RT. The cells were then centrifuged at 2000 xg for 5 minutes at RT. The cells 794  
724 were resuspended in 1 mL of PBS and centrifuged again at 2000 xg for 5 min- 795  
725 utes at RT. Hybridization of new fluorescent oligonucleotides was carried out as 796  
726 described above. 797

#### 727 **Stain Index calculation**

728 The Stain Index (SI) was calculated by measuring the geometric mean of the 798  
729 positive and negative populations as well as the standard deviation of the nega- 799  
730 tive population using FlowJo Software. The SI was calculated as follows:  $(Geo.$  800  
731  $Mean_{POS} - Geo. Mean_{NEG}) / (2 \times SD_{NEG})$ . 801

#### 732 **Live cell RNA sequencing**

733 *In vivo* retina electroporation was carried out as described previously at P2<sup>10</sup>. 802  
734 Two plasmids, CAG-BFP and Grik1<sup>CRM4</sup>-GFP, were electroporated simultane- 803  
735 ously at a concentration of 1  $\mu$ g/ $\mu$ L per plasmid. Retinas were harvested at P40. 804  
736 The electroporated and unelectroporated regions were processed separately. The 805  
737 electroporated region was dissociated as described above, and BFP<sup>+</sup>/GFP<sup>+</sup> cells 806  
738 were FACS isolated into Trizol (Thermo Fisher Scientific, cat. #15596026). 807  
739 Cells from the unelectroporated region were used for Probe-Seq as described 808  
740 above. The RNA from the cells in Trizol was extracted following manufacturers 809  
741 protocol. The RNA-sequencing libraries were generated using the SMART-Seq 810  
742 v.4 and Nextera XT kits as described above. 811

#### 743 **Histology and SABER FISH**

744 For the mouse retina, adult CD1 mouse retinas were dissected and fixed in 812  
745 4% PFA for 20 minutes at RT. The fixed retinas were cryoprotected in 30% 813  
746 sucrose (in PBS). Once submerged, the samples were embedded in 50%/15% 814  
747 OCT/Sucrose mixture in an ethanol/dry ice bath and stored at -80°C. The reti- 815  
748 nas were cryosectioned at 15  $\mu$ M thickness. For the human eye, formalin- 816  
749 fixed human postmortem eyes were obtained from Restore Life USA. Patient 817  
750 DRLU101818C was a 54-year-old male with no clinical eye diagnosis and the 818  
751 postmortem interval was 4 hours. Patient DRLU110118A was a 59-year-old fe- 819  
752 male with no clinical eye diagnosis and the postmortem interval was 4 hours. A 820  
753 square (1 cm x 1 cm) of the human retina was cryoprotected, embedded, and 821  
754 cryosectioned as described above. For the *Drosophila* gut, the midgut was fixed 822  
755 in 4% PFA for 30 minutes at RT. For the chick retina, the central region of de- 823  
756 veloping HH28 chick retina that contained the developing high acuity area was 824  
757 excised and fixed in 4% PFA for 20 minutes at RT. The retina was then cryopro- 825  
758 tected, embedded as described above, and cryosectioned at 50  $\mu$ M thickness. 826  
759 827

760 SABER FISH of retinal sections was carried out on Superfrost Plus slides 828  
761 (Thermo Fisher Scientific, cat. #1255015) using an adhesive hybridization 829  
762 chamber (Grace Bio-Labs, cat. #621502). For *Drosophila* guts, wholemount 830  
763 SABER FISH was performed in microcentrifuge tubes. For retinal sections, they 831  
764 were rehydrated with PBS for 5-10 minutes to remove the OCT on the slides. 832

Subsequently, sections were completely dried to adhere the sections to the slides. 764  
Once dry, the adhesive chamber was placed to encase the sections. For both reti- 765  
nal sections and wholemount *Drosophila* guts, the samples were incubated in 766  
0.1% PBS/Tween-20 (MilliporeSigma, cat. #P9416) for at least 10 minutes. The 767  
PBST was removed, and the samples were incubated with pre-warmed (43°C) 768  
40% wHyb (2x SSC, 40% deionized formamide, 1% Tween-20, diluted in Ul- 769  
traPure Water) for at least 15 minutes at 43°C. The 40% wHyb was removed, 770  
and the samples were then incubated with 100  $\mu$ L of pre-warmed (43°C) Probe 771  
Mix (1  $\mu$ g of probe per gene, 96  $\mu$ L of Hyb1 solution (2.5x SSC, 50% deionized 772  
formamide, 12.5% Dextran Sulfate, 1.25% Tween-20), diluted up to 120  $\mu$ L 773  
with UltraPure Water) and incubated 16-48 hours at 43°C. The samples were 774  
washed twice with 40% wHyb (30 minutes/wash, 43°C), twice with 2x SSC 775  
(15 minutes/wash, 43°C), and twice with 0.1% PBST (5 minutes/wash, 37°C). 776  
The samples were then incubated with 100  $\mu$ L of Fluorescent Oligonucleotide 777  
Mix (100  $\mu$ L of PBST, 2  $\mu$ L of each 10  $\mu$ M Fluorescent Oligonucleotide) for 778  
15 minutes at 37°C. The samples were washed three times with PBST at 37°C 779  
for 5 minutes each and counterstained with DAPI (Thermo Fisher Scientific, cat. 780  
#D1306; 1:50,000 of 5 mg/mL stock solution in PBS) or WGA-405s (Biotium, 781  
cat. #290271; 1:100 of 1 mg/mL stock solution in PBS). Cell segmentation and 782  
cell calling algorithms were performed as described previously<sup>24</sup>. 783

#### 784 **Imaging**

785 Fluorescent images were acquired with W1 Yokogawa Spinning disk confocal 786  
787 microscope with 50  $\mu$ M pinhole disk and 488, 561, and 640 laser lines. The ob- 788  
789 jectives used were either Plan Fluor 40x/1.3 or Plan Apo 60x/1.4 oil objectives, 790  
and the camera used was Andor Zyla 4.2 Plus sCMOS monochrome camera. 791  
Nikon Elements Acquisition Software (AR 5.02) was used for image acquisition 792  
and Fiji or Adobe Photoshop CS6 was used for image analysis. SABER FISH 793  
images were acquired as a z-stack and converted to a 2D image by maximum 794  
projection in Fiji. 795

#### 796 **Data availability**

797 Raw sequencing data and matrices of read counts for the mouse, chick, and 798  
799 *Drosophila* Probe-Seq are available at GEO: GSE135572. 800

#### 801 **Code availability**

802 All R scripts used for differential expression analysis are available in Supple- 803  
804 mentary Files. 805

#### 806 **REFERENCES**

- 807 1. Sanes, J.R. & Zipursky, S.L. Design principles of insect and vertebrate visual 808  
809 systems. *Neuron* 66, 15-36 (2010). 810
- 811 2. Vlasits, A.L., Euler, T. & Franke, K. Function first: classifying cell types and 812  
813 circuits of the retina. *Current opinion in neurobiology* 56, 8-15 (2019). 814
- 815 3. Macosko, E.Z. et al. Highly Parallel Genome-wide Expression Profiling of 816  
817 Individual Cells Using Nanoliter Droplets. *Cell* 161, 1202-1214 (2015). 818
- 819 4. Rheaume, B.A. et al. Single cell transcriptome profiling of retinal ganglion 820  
821 cells identifies cellular subtypes. *Nature communications* 9, 2759 (2018). 822
- 823 5. Shekhar, K. et al. Comprehensive Classification of Retinal Bipolar Neurons 824  
825 by Single-Cell Transcriptomics. *Cell* 166, 1308-1323 (2016). 826
- 827 6. Consortium, T. et al. Single-cell transcriptomics of 20 mouse organs creates 828  
829 a Tabula Muris. *Nature* 562, 367-372 (2018). 830
- 831 7. Han, X. et al. Mapping the Mouse Cell Atlas by Microwell-Seq. *Cell* 172, 832  
833 1091-1107 (2018). 834
- 835 8. Regev, A. et al. The Human Cell Atlas. *eLife* 6 (2017). 836
- 837 9. Arlotta, P. et al. Neuronal subtype-specific genes that control corticospinal 838  
839 motor neuron development *in vivo*. *Neuron* 45, 207-221 (2005). 840
- 841 10. Matsuda, T. & Cepko, C.L. Controlled expression of transgenes introduced 842  
843 by *in vivo* electroporation. *Proceedings of the National Academy of Sciences of the* 844  
845 *United States of America* 104, 1027-1032 (2007). 846
- 847 11. Molyneaux, B.J. et al. DeCoN: genome-wide analysis of *in vivo* transcrip- 848  
849 tional dynamics during pyramidal neuron fate selection in neocortex. *Neuron* 850  
851 85, 275-288 (2015). 852
- 853 12. Siegart, S. et al. Transcriptional code and disease map for adult retinal cell 854  
855 types. *Nature neuroscience* 15, 487-495 (2012). 856
- 857 13. Telley, L. et al. Sequential transcriptional waves direct the differentiation 858  
859 of newborn neurons in the mouse neocortex. *Science (New York, N.Y.)* 351, 860  
861 1443-1446 (2016). 862
- 863 14. Xu, X. et al. Species and cell-type properties of classically defined human 864  
865 and rodent neurons and glia. *eLife* 7 (2018). 866
- 867 15. Jaitin, D.A. et al. Massively parallel single-cell RNA-seq for marker-free de- 868  
869 composition of tissues into cell types. *Science (New York, N.Y.)* 343, 776-779 870  
871 (2014). 872



- 833 16. Klein, A.M. et al. Droplet barcoding for single-cell transcriptomics applied to embryonic stem cells. *Cell* 161, 1187-1201 (2015). 888
- 834 17. Picelli, S. et al. Smart-seq2 for sensitive full-length transcriptome profiling in single cells. *Nature methods* 10, 1096-1098 (2013). 889
- 835 18. Shalek, A.K. et al. Single-cell transcriptomics reveals bimodality in expression and splicing in immune cells. *Nature* 498, 236-240 (2013). 890
- 836 19. Amamoto, R. et al. FIN-Seq: Transcriptional profiling of specific cell types in frozen archived tissue from the human central nervous system. *bioRxiv*, 602847 (2019). 891
- 837 20. Hrvatin, S., Deng, F., O'Donnell, C.W., Gifford, D.K. & Melton, D.A. MARIS: method for analyzing RNA following intracellular sorting. *PLoS one* 9 (2014). 892
- 838 21. Pan, Y., Ouyang, Z., Wong, W.H. & Baker, J.C. A new FACS approach isolates hESC derived endoderm using transcription factors. *PLoS one* 6 (2011). 893
- 839 22. Pechhold, S. et al. Transcriptional analysis of intracytoplasmically stained, FACS-purified cells by high-throughput, quantitative nuclease protection. *Nature biotechnology* 27, 1038-1042 (2009). 894
- 840 23. Yamada, H. et al. Messenger RNA quantification after fluorescence activated cell sorting using intracellular antigens. *Biochemical and Biophysical Research Communications* 397, 425-428 (2010). 895
- 841 24. Kishi, J.Y. et al. SABER amplifies FISH: enhanced multiplexed imaging of RNA and DNA in cells and tissues. *Nature methods* 16, 533-544 (2019). 896
- 842 25. Klemm, S. et al. Transcriptional profiling of cells sorted by RNA abundance. *Nature methods* 11, 549-551 (2014). 897
- 843 26. Maeda, T. et al. Optimization of Recovery and Analysis of RNA in Sorted Cells in mRNA Quantification After Fluorescence-activated Cell Sorting. *Annals of clinical and laboratory science* 46, 571-577 (2016). 898
- 844 27. Yamada, H. et al. Messenger RNA quantification after fluorescence-activated cell sorting using *in situ* hybridization. *Cytometry. Part A: the journal of the International Society for Analytical Cytology* 77, 1032-1037 (2010). 899
- 845 28. Kishi, J.Y., Schaus, T.E., Gopalkrishnan, N., Xuan, F. & Yin, P. Programmable autonomous synthesis of single-stranded DNA. *Nature chemistry* 10, 155-164 (2018). 900
- 846 29. Sigurgeirsson, B., Emanuelsson, O. & Lundberg, J. Sequencing degraded RNA addressed by 3' tag counting. *PLoS one* 9 (2014). 901
- 847 30. Krishnaswami, S.R. et al. Using single nuclei for RNA-seq to capture the transcriptome of postmortem neurons. *Nature protocols* 11, 499-524 (2016). 902
- 848 31. Lake, B.B. et al. Neuronal subtypes and diversity revealed by single-nucleus RNA sequencing of the human brain. *Science (New York, N.Y.)* 352, 1586-1590 (2016). 903
- 849 32. Cowan, C.S. et al. Cell types of the human retina and its organoids at single-cell resolution: developmental convergence, transcriptomic identity, and disease map. *bioRxiv*, 703348 (2019). 904
- 850 33. Dutta, D. et al. Regional Cell-Specific Transcriptome Mapping Reveals Regulatory Complexity in the Adult *Drosophila* Midgut. *Cell reports* 12, 346-358 (2015). 905
- 851 34. Hung, R.-J. et al. A cell atlas of the adult *Drosophila* midgut. *bioRxiv*, 410423 (2018). 906
- 852 35. Doup, D.P., Marshall, O.J., Dayton, H., Brand, A.H. & Perrimon, N. *Drosophila* intestinal stem and progenitor cells are major sources and regulators of homeostatic niche signals. *Proceedings of the National Academy of Sciences of the United States of America* 115, 12218-12223 (2018). 907
- 853 36. Bruhn, S.L. & Cepko, C.L. Development of the pattern of photoreceptors in the chick retina. *The Journal of neuroscience: the official journal of the Society for Neuroscience* 16, 1430-1439 (1996). 908
37. da Silva, S. & Cepko, C.L. Fgf8 Expression and Degradation of Retinoic Acid Are Required for Patterning a High-Acuity Area in the Retina. *Developmental cell* 42, 68-81 (2017). 909
38. Eastburn, D.J., Sciambi, A. & Abate, A.R. Identification and genetic analysis of cancer cells with PCR-activated cell sorting. *Nucleic acids research* 42 (2014). 910
39. Pellegrino, M. et al. RNA-Seq following PCR-based sorting reveals rare cell transcriptional signatures. *BMC genomics* 17, 361 (2016). 911
40. Rouhanifard, S.H. et al. ClampFISH detects individual nucleic acid molecules using click chemistry-based amplification. *Nature biotechnology* 37, 84-89 (2018). 912
41. Wang, F. et al. RNAscope: a novel *in situ* RNA analysis platform for formalin-fixed, paraffin-embedded tissues. *The Journal of molecular diagnostics: JMD* 14, 22-29 (2012). 913
42. Alles, J. et al. Cell fixation and preservation for droplet-based single-cell transcriptomics. *BMC biology* 15, 44 (2017). 914
43. Attar, M. et al. A practical solution for preserving single cells for RNA sequencing. *Scientific reports* 8, 2151 (2018). 915
44. Chen, J. et al. PBMC fixation and processing for Chromium single-cell RNA sequencing. *Journal of translational medicine* 16, 198 (2018). 916
45. Hamburger, V. & Hamilton, H.L. A series of normal stages in the development of the chick embryo. *Journal of morphology* 88, 49-92 (1951). 917
46. Aken, B.L. et al. Ensembl 2017. *Nucleic acids research* 45 (2017). 918
47. Dobin, A. et al. STAR: ultrafast universal RNA-seq aligner. *Bioinformatics (Oxford, England)* 29, 15-21 (2013). 919
48. Okonechnikov, K., Conesa, A. & Garcia-Alcalde, F. Qualimap 2: advanced multi-sample quality control for high-throughput sequencing data. *Bioinformatics (Oxford, England)* 32, 292-294 (2016). 920
49. Anders, S., Pyl, P.T. & Huber, W. HTSeq—a Python framework to work with high-throughput sequencing data. *Bioinformatics (Oxford, England)* 31, 166-169 (2015). 921
50. Love, M.I., Huber, W. & Anders, S. Moderated estimation of fold change and dispersion for RNA-seq data with DESeq2. *Genome biology* 15, 550 (2014). 922
51. Subramanian, A. et al. Gene set enrichment analysis: a knowledge-based approach for interpreting genome-wide expression profiles. *Proceedings of the National Academy of Sciences of the United States of America* 102, 15545-15550 (2005). 923
- Acknowledgments:** We would like to thank former and current members of the Cepko and Tabin Labs for the insightful discussion and feedback. We thank P.M. Llopis, R. Stephansky, and the MicRoN core at Harvard Medical School for their assistance with microscopy. We thank C. Araneo, F. Lopez, and the Flow Cytometry Core Facility for their assistance with flow cytometry. We thank S. da Silva for providing the image of *in situ* hybridization for FGF8 in the developing chick retina. We thank C. Cowan and B. Roska for providing the list of human retinal cell type-specific markers. This work was supported by the Howard Hughes Medical Institute (C.L.C. and N.P.), Edward R. and Anne G. Lefler Postdoctoral Fellowship (R.A.), and HSCI Internship Program (M.D.G.). 924
- Author Contributions:** R.A., E.R.W., S.W.L., and C.L.C. conceived the study and designed the experiments. R.A. executed the experiments and analyzed the data. M.G. contributed to the execution of the frozen nuclei protocol. E.R.W. performed the analysis of puncta quantification and stain index. J.C. provided the chick tissue. E.A.L. and N.P. provided the *Drosophila* tissue. R.A. and C.L.C. wrote the manuscript, and all authors edited the manuscript. C.L.C. supervised all aspects of the work. 925
- Competing interests:** The authors declare no conflict of interest. 926